Supporting Information

Romanino et al. 10.1073/pnas.1111448109

SI Materials and Methods

Quantitative Real-Time PCR. Total RNA was isolated (SV Total RNA Isolation System; Promega), and equal amounts of RNA were reverse transcribed using a mixture of oligodT and random hexamer primers (iScript cDNA Synthesis Kit; Bio-Rad). Quantitative real-time PCR (qRT-PCR) was performed using SYBR Green (PowerSYBR Green Master Mix; Applied Biosystems) and StepOne Software 2.1. (Applied Biosystems). Expression levels for each gene of interest were normalized to the mean cycle number using qRT-PCR for the housekeeping gene GAPDH. All data were confirmed with β-actin as another housekeeping gene. For the qRT-PCR data of the mTOR^{-} mice the housekeeping genes cyclophilin B and hypoxanthine phosphoribosyltransferase (HPRT) were used.

For qRT-PCR the following primers were used: GAPDH (forward: CAT CGT GGA AGG GCT CAT GAC, reverse: CTT GGC AGC ACC AGT GGA TG); cyclophilin B (forward: GAT GGC ACA GGA GGA AAG AG, reverse: AAC TTT GCC GAA AAC CAC AT); β-actin (forward: CAG CTT CTT TGC AGC TCC TT, reverse: GCA GCG ATA TCG TCA TCC A); peroxisome proliferator-activated receptor gamma coactivator 1-α (PGC-1α; forward: TGA TGT GAA TGA CTT GGA TAC AGA CA, reverse: GCT CAT TGT TGT ACT GGT TGG ATA TG); peroxisome proliferator-activated receptor α (PPARα; forward: GCG TAC GGC AAT GGC TTT AT, reverse: ACA GAA CGG CTT CCT CAG GTT); PPARδ (forward: GCA AGC CCT TCA GTG ACA TCA, reverse: CCA GCG CAT TGA ACT TGA CA); medium-chain acyl CoA dehydrogenase (MCAD; forward: AAC ACT TAC TAT GCC TCG ATT GCA, reverse: CCA TAG CCT CCG AAA ATC TGA A); cytochrome *c* (forward: GCA AGC ATA AGA CTG GAC CAA A, reverse: TTG TTG GCA TCT GTG TAA GAG AAT C); cytochrome *c* oxidase IV(COX IV; forward: TAC TTC GGT GTG CCT TCG A, reverse: TGA CAT GGG CCA CAT CAG); citrate synthase (forward: CAA GCA GCA ACA TGG GAA GA, reverse: GTC AGG ATC AAG AAC CGA AGT CT); glycogen phosphorylase (GP; forward: CAC TTA CCA GCT GGG CTT GGA CAT, reverse: AAA GCA AGC TGC CAG GCG TC); COX I (forward: GGT CAA CCA GGT GCA CTT TT, reverse: TGG GGC TCC GAT TAT TAG TG); long-chain acyl-CoA dehydrogenase (LCAD; forward: ATG GCA AAA TAC TGG GCA TC, reverse: TCT TGC GAT CAG CTC TTT CA); muscle carnitine palmitoyltransferase I (mCPT1; forward: TGC CTT TAC ATC GTC TCC AA, reverse: AGA CCC CGT AGC CAT CAT C); dystrophin (forward: TGC GCT ATC AGG AGA CAA TG, reverse: TTC TTG GCC ATC TCC TTC AC); myogenin (forward: CTA CAG GCC TTG CTC AGC TC, reverse: AGA TTG TGG GCG TCT GTA GG); and myosin heavy-chain 8 (MyH8; forward: CAA GGA TGG AGG GAA AGT GA, reverse: GGT TCA TGG GGA AGA CTT GA).

For the quantification of mtDNA copy numbers the following primers were used: *D-loop* region (forward: GGT TCT TAC TTC AGG GCC ATC A, reverse: GAT TAG ACC CGT TAC CAT CGA GAT), NADH dehydrogenase (ubiquinone) flavoprotein 1 (*Ndufv1*; forward: CTT CCC CAC TGG CCT CAA G, reverse: CCA AAA CCC AGT GAT CCA GC).

Succinate Dehydrogenase Activity. Frozen muscles were homogenized in medium containing 50% glycerol, 20 mM phosphate buffer (pH 7.4), 5 mM β-mercaptoethanol, 0.5 mM EDTA, and 0.02% BSA at a dilution of 1:50 based on wet weight. Succinate dehydrogenase activity was determined at 37 °C in a two-step assay as described (1). In the first step, fumarate was allowed to accumulate from succinate for 60 min. In the second step, the amount of fumarate produced was measured with fumarase and a NAD-coupled reaction with malate dehydrogenase and the glutamate-oxaloacetate transaminase. The amount of NADH produced was measured by its fluorescence. Standards were processed the same way as the samples.

Histology. Muscles frozen in liquid nitrogen-cooled isopentane were cut into 12-μm cross-sections. General histology on cross-sections was performed using H&E (Merck). NADH staining was done as described (2). PAS staining was performed according to the manufacturer's instructions (Sigma). After staining, samples were dehydrated and mounted with DePex mounting medium (Gurr; BDH Chemicals, Ltd.). SDH and COX staining were carried out as described in refs. 3 and 4.

Quantification of mtDNA Copy Numbers. Total DNA was extracted and purified with a standard chloroform/ethanol precipitation after proteinase K digestion. DNA concentrations were determined photometrically, adjusted to 50 ng/μL, and used to quantify the amount of mtDNA in relation to the genomic DNA by qRT-PCR. For the quantification of the mtDNA, primers were used that are complementary to the *D-loop* region. Primers to quantify genomic DNA were directed against the single-copy nuclear gene *Ndufv1*.

Electron Microscopy. Transmission electron microscopy was performed as described in ref. 5.

Western Blotting Analysis, Glycogen Content, and Fiber Size Distribution. Western blotting, glycogen content, and fiber size distribution were performed as described earlier (6). For Western blots the following antibodies were used: anti–PGC-1 from Millipore; Pan-actin, Akt, phospho-Akt (Thr308), phospho-Akt (Ser473), glycogen synthase kinase 3β (GSK-3β), Phospho-GSK-3β (Ser9), and raptor from Cell Signaling; α-actinin from Sigma; and GP from Santa Cruz. The concentrations used were according to the manufacturers' instructions.

Voluntary Wheel Running. Mice were housed individually in cages equipped with a running wheel carrying a magnet. Wheel revolutions were registered by a reed sensor connected to an I-7053D Digital-Input module (Spectra), and the revolution counters were read by a standard laptop computer via an I-7520 RS-485-to-RS-232 interface converter (Spectra). Digitalized signals were processed by the "mouse running" software developed by Santhera Pharmaceuticals Ltd.

Physiological Studies. Measurements of muscle contractile properties of the soleus and tibialis anterior (TA) muscle (Table S1) were performed as described (7). Muscle force of extensor digitorum longus (EDL) muscles (Table S4) was measured as described previously (8) using a muscle-testing setup (Heidelberg Scientific Instruments). Tetanic force was recorded in response to 400-ms pulses at 150 Hz, and specific force was normalized to the muscle cross-sectional area [CSA = wet weight (mg)/length (mm) × 1.06 (density mg/mm^3)].

1. Chi MM, et al. (1983) Effects of detraining on enzymes of energy metabolism in individual human muscle fibers. *Am J Physiol* 244:C276–C287.
2. Dunant P, et al. (2003) Expression of dystrophin driven by the 1.35-kb MCK promoter ameliorates muscular dystrophy in fast, but not in slow muscles of transgenic mdx mice. *Mol Ther* 8:80–89.
3. Konieczny P, et al. (2008) Myofiber integrity depends on desmin network targeting to Z-disks and costameres via distinct plectin isoforms. *J Cell Biol* 181:667–681.
4. MacArthur DG, et al. (2007) Loss of ACTN3 gene function alters mouse muscle metabolism and shows evidence of positive selection in humans. *Nat Genet* 39:1261–1265.
5. Moll J, et al. (2001) An agrin minigene rescues dystrophic symptoms in a mouse model for congenital muscular dystrophy. *Nature* 413:302–307.
6. Bentzinger CF, et al. (2008) Skeletal muscle-specific ablation of raptor, but not of rictor, causes metabolic changes and results in muscle dystrophy. *Cell Metab* 8: 411–424.
7. Risson V, et al. (2009) Muscle inactivation of mTOR causes metabolic and dystrophin defects leading to severe myopathy. *J Cell Biol* 187:859–874.
8. Delbono O, et al. (2007) Loss of skeletal muscle strength by ablation of the sarcoplasmic reticulum protein JP45. *Proc Natl Acad Sci USA* 104:20108–20113.

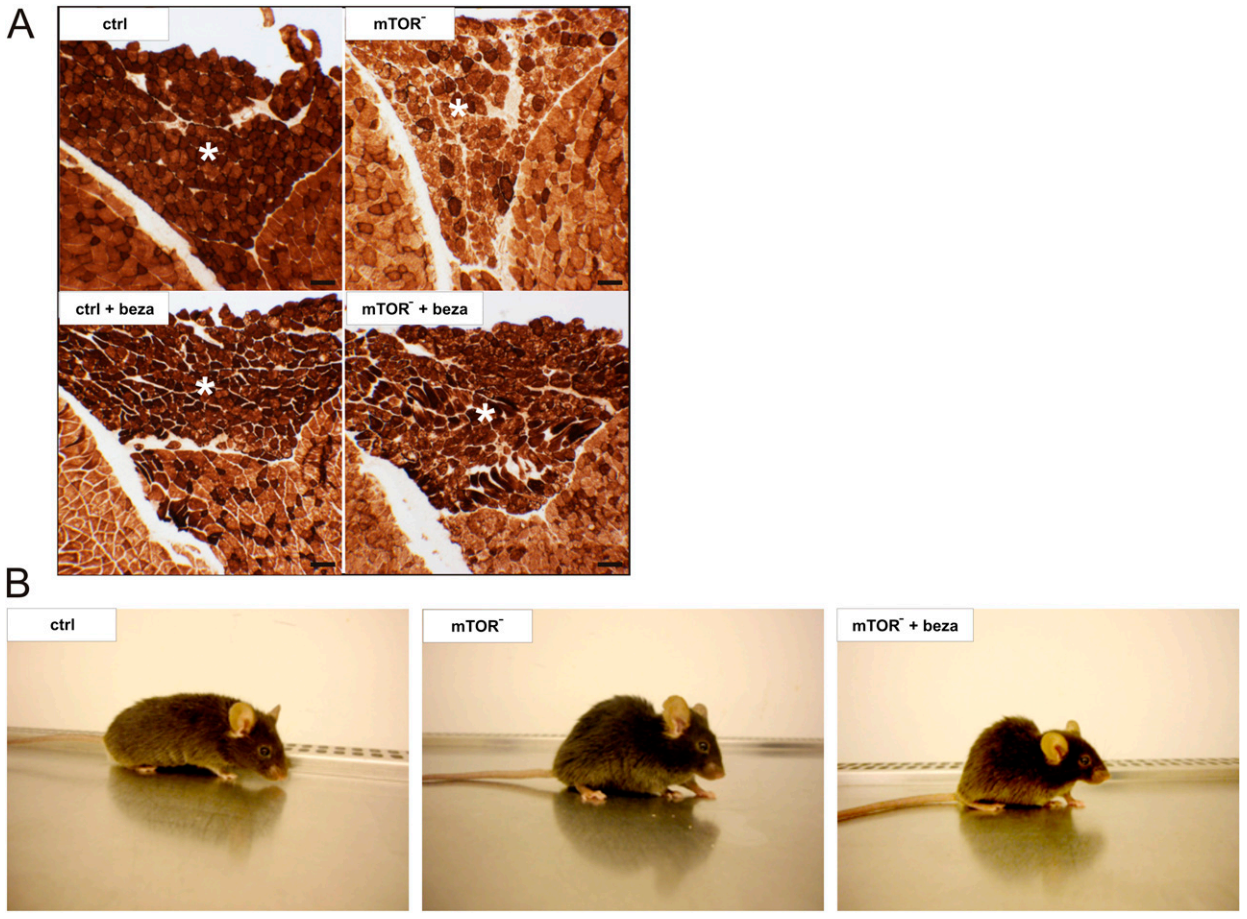

Fig. S1. Oxidative properties and myopathy in bezafibrate-treated control and mTOR^{-} mice. (*A*) COX staining in hind leg muscles. COX is the complex IV of the respiratory chain enzymes, and its activity is representative for the oxidative enzymes. The soleus muscle is marked by an asterisk. (Scale bar, 100 μm.) (*B*) Photographs of 140-d-old mice of indicated genotypes. Note that bezafibrate-treated mTOR^{-} mice still develop a severe kyphosis.

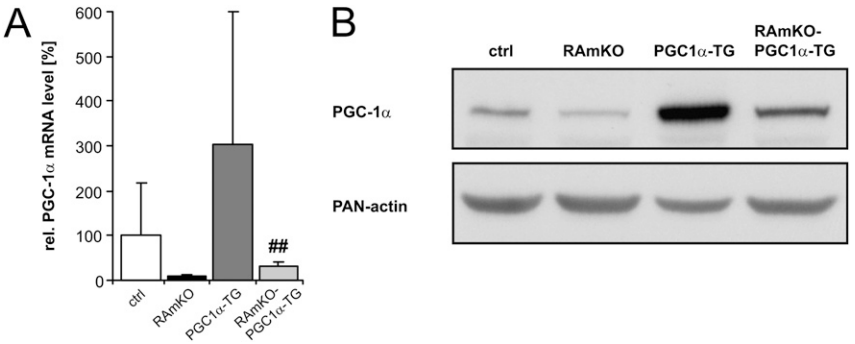

Fig. S2. Transgenic expression of PGC-1α in control and raptor muscle-knockout (RAmKO) mice. (*A*) Relative mRNA levels of PGC-1α in soleus muscle of 90-d-old mice as determined by qRT-PCR. Values represent mean ± SD ($n \geq 6$ mice). $^{\#\#}P < 0.01$, RAmKO vs. RAmKO mice that also are transgenic for PGC1α (RAmKO-PGC1α-TG mice). (*B*) Western blot of PGC-1α in EDL muscles from 80-d-old mice. Equal amounts of protein were loaded in each lane. An antibody against Pan-actin was used as loading control. For quantification, see Fig. 2*B*.

Table S1. Muscle contractile properties of 140-d-old mice were assessed by recording isometric forces in response to electrical stimulation

Muscle	Control	mTOR$^-$	mTOR$^-$ + beza
Soleus			
Mass (mg)	13.2 ± 1.6	9.7 ± 1***	7.0 ± 0.3*** ###
Po (mN)	224.2 ± 52.2	132.0 ± 19.9**	104.8 ± 9.7** #
sPo (mN/mm^2)	171.2 ± 40.2	130.6 ± 14.5*	140.0 ± 17.2*
TA			
Mass (mg)	61.5 ± 5.1	38.3 ± 6.9***	26.9 ± 2.3*** ##
Po (mN)	1137.3 ± 118.7	445.8 ± 118.4**	292.3 ± 75.8***
sPo (mN/mm^2)	18.5 ± 0.7	11.8 ± 1.1***	11.3 ± 2.4***
Pt (mN)	20.7 ± 3.3	7.2 ± 1.8***	3.3 ± 0.7*** ##

The following data were measured: muscle mass (Mass), absolute maximum tetanic force (Po), specific tetanic force (sPo), and peak twitch tension (Pt). Data represent mean ± SD ($n \geq 3$ mice). Significant differences between control and experimental groups are indicated by *; significant changes between mTOR$^-$ and bezafibrate mTOR$^-$ (mTOR$^-$ + beza) mice are indicated by #. *P* values were determined by Student's *t* test. $^{*/\#}P < 0.05$; $^{**/\#\#}P < 0.01$; $^{***/\#\#\#}P < 0.001$.

Table S2. Quantification of Western blot analysis for the proteins indicated

Protein	Control	RAmKO	PGC1α-TG	RAmKO-PGC1α-TG
Raptor	100.0 ± 63.9	0.9 ± 1.5**	44.2 ± 25.3	3.3 ± 2.7**
total PKB/Akt	100.0 ± 19.8	252.6 ± 43.9	318.8 ± 92.1	520.6 ± 205.5** #
P-PKB/Akt T308	100.0 ± 10.9	393.7 ± 14.2**	66.2 ± 44.6	236.5 ± 47.5**
P-PKB/Akt S473	100.0 ± 113.7	1192.7 ± 15.7**	52.5 ± 32.3	1696.9 ± 458.7**
GSK3β	100.0 ± 35.7	98.0 ± 0.7	58.1 ± 26.2	133.2 ± 40.5
P-GSK3β S9	100.0 ± 37.8	294.1 ± 159.2*	61.7 ± 37.3	233.4 ± 113.1*
GP	100.0 ± 47.5	4.5 ± 0.9**	20.1 ± 10.4*	7.7 ± 4.3**

Proteins analyzed were extracted from EDL muscle of 80-d-old mice ($n \geq 3$ mice). Numbers given represent mean gray value ± SD after subtraction of the background and normalization to α-actinin. Significant differences between control and genetically modified mice are indicated by *; significant changes between RAmKO and RAmKO-PGC1α-TG mice are indicated by #. $^{*/\#}P < 0.05$; $^{**/\#\#}P < 0.01$; $^{***/\#\#\#}P < 0.001$.

Table S3. Weight or length measured for different organs in 140-d-old mice

Muscle or organ	Control	RAmKO	PGC1α-TG	RAmKO-PGC1α-TG
Soleus (mg)	8.1 ± 0.6	6.6 ± 0.8*	8.6 ± 0.8	6.3 ± 0.6**
EDL (mg)	11.4 ± 1.2	10.6 ± 0.5	11.1 ± 1.3	9.8 ± 1.2
TA (mg)	48.4 ± 3.9	41.8 ± 4.5*	50.9 ± 3.9	35.2 ± 4.4** #
Heart (mg)	147.2 ± 16.4	126.9 ± 4.8	154.8 ± 11.9	136.3 ± 7.9
Liver (mg)	1281.2 ± 338.7	1212.3 ± 139.8	1345.3 ± 140.3	1183.9 ± 161.1
Tibia length (cm)	2.1 ± 0.1	2.1 ± 0.1	2.0 ± 0.1	2.0 ± 0.1

Values represent mean ± SD ($n \geq 6$ mice). Significant differences between control and genetically modified mice are indicated by *; significant changes between RAmKO and RAmKO-PGC1α-TG mice are indicated by #. $^{*/\#}P < 0.05$; $^{**/\#\#}P < 0.01$; $^{***/\#\#\#}P < 0.001$.

Table S4. Muscle contractile properties of EDL muscle of 90-d-old mice were assessed by recording isometric forces in response to electrical stimulation

EDL properties	Control	RAmKO	PGC1α-TG	RAmKO-PGC1α-TG
Mass (mg)	9.8 ± 2.1	9.2 ± 1.3	9.4 ± 2.2	8.2 ± 1.2
Po (mN)	282.3 ± 54.5	237.6 ± 47.9*	217.6 ± 47.2*	192.3 ± 8.9**
sPo (mN/mm^2)	358.4 ± 55.5	309.0 ± 72.6*	299.1 ± 52.3*	280.8 ± 27.7*
Pt (mN)	51.3 ± 14.0	43.8 ± 12.7	30.4 ± 11.5**	31.3 ± 7.4*

The following data were measured: muscle mass (Mass), absolute maximum tetanic force (Po), specific tetanic force (sPo), and peak twitch tension (Pt). Values represent mean ± SD ($n \geq 4$ muscles). In agreement with recent findings of others (1), EDL muscles from PGC-1α-TG mice are significantly weaker than EDL muscles from controls, Significant differences between control and genetically modified mice are indicated by *; significant changes between RAmKO and RAmKO-PGC1α-TG mice are indicated by #. *P* values were determined by Student's *t* test. $^{*/\#}P < 0.05$; $^{**/\#\#}P < 0.01$; $^{***/\#\#\#}P < 0.001$.

1. Summermatter S, et al. (2011) Remodeling of calcium handling in skeletal muscle through PGC-1{alpha}: Impact on force, fatigability and fiber type. *Am J Physiol Cell Physiol*.